Article

Kinetics and Thermodynamics of Amyloid Fibril Assembly

Ronald Wetzel

Acc. Chem. Res., **2006**, 39 (9), 671-679• DOI: 10.1021/ar050069h • Publication Date (Web): 22 July 2006

Kinetics and Thermodynamics of Amyloid Fibril Assembly

RONALD WETZEL*
Graduate School of Medicine, University of Tennessee, 1924 Alcoa Highway, Knoxville, Tennessee 37920

Received February 3, 2006

ABSTRACT
With some exceptions, amyloids appear to be accidental aggregated structures whose formation was not selected for in molecular evolution. Despite this, amyloid fibrils are in many respects surprisingly well-behaved molecules. For example, Huntington's disease-related polyglutamine sequences aggregate via a relatively simple nucleated growth polymerization mechanism. In addition, the Alzheimer's plaque protein Aβ has been shown to undergo reversible amyloid fibril formation to a position of dynamic equilibrium such that reaction thermodynamics can be quantified. Studies of these well-behaved amyloid systems are allowing us to peer more deeply into the process and products of off-pathway misfolding and aggregation.

Off-pathway protein aggregation has in recent years become recognized as an important, and previously neglected, aspect of the protein folding landscape. Results of genetics experiments[1] are consistent with a major role for aggregation in guiding the molecular evolution of proteins, and the existence of a variety of systems for managing and, in most cases, avoiding or suppressing this process[2] suggests that aggregation plays a role in the everyday lives of cells and organisms. In biotechnology, off-pathway aggregation is also normally undesirable, representing significant barriers to protein expression[3] and recovery.[4] Protein aggregates are associated with a variety of human diseases.[5,6] At the same time, aggregates can sometimes be desirable. Some amyloids, for example, appear to result from evolved pathways (yielding "on-pathway aggregates") and serve a useful role to their host.[7] Designed amyloids may ultimately have a role as nanomaterials.

Despite the extraordinary importance of understanding protein aggregation and aggregates, however, detailed biophysical studies have proved elusive, perhaps simply because most of the techniques and conceptualizations of protein folding research are built around solution phase transformations. As a place to focus initial biophysical studies on protein aggregation, amyloid fibril formation is particularly attractive: first, because most of the protein folding disorders described to date appear to involve amyloid fibrils or amyloid-related aggregates;[5,6] second, because amyloid appears to be a particularly well-behaved version of off-pathway aggregation featuring relatively well-defined repeat structures. This not only allows for interpretable ensemble measurements but also means that the aggregates might behave in some respects like folded proteins and might thus be analyzed using similar techniques and mathematical approaches. Amyloid also appears to be a reasonable exemplar of off-pathway aggregates, which in general tend to be rich in β-sheet and relatively stable and insoluble in aqueous buffers.[8]

Deducing molecular mechanisms typically requires studies on the structures of reactants, intermediates, and products, and on the kinetics and thermodynamics of their interconversions. Off-pathway aggregate formation by globular proteins is particularly difficult and complex to study at this level owing to the transient nature of the aggregation-prone species. For example, both in classical protein aggregation and in amyloid formation, aggregation proceeds efficiently only under conditions where the native state is destabilized.[9] Owing to the potentially transient nature of the aggregating species, folding kinetics can also play a major role, both during protein folding[1] and during unfolding.[10] Even after the kinetic and thermodynamic requirements for the generation of the aggregation-prone state are factored out, however, amino acid sequence continues to play an important role by controlling the intimate packing interactions mediating protein self-assembly into kinetically favored and thermodynamically stable non-native states.[9]

Given the above considerations, it would appear that an especially attractive line of research would be one that involves systems whose starting points are relatively disordered monomeric peptides and whose endpoints are regularly packed amyloid aggregates. Our lab has focused on two disease-related examples of this type of amyloidogenic peptide, Aβ peptide as found in Alzheimer's disease plaques[11] and polyglutamine peptides as found in expanded CAG repeat diseases such as Huntington's disease.[12] In this Account, we show that it is possible to extract kinetics and thermodynamic data on aggregation that can be interpreted in terms of details of aggregate structure and assembly mechanisms, in much the same manner that has become standard fare for globular protein folding studies. The results make possible new insights into the assembly pathways and structures of off-pathway aggregates and new clues to pathology.

Kinetics of Amyloid Formation

Spontaneous formation of amyloid fibrils from disordered peptides is often discussed as a version of a nucleated growth polymerization pathway.[13] In this mechanism, the overall rate of amyloid formation is limited by the slow generation of nuclei (the nucleation phase), which, once formed, rapidly grow by monomer addition to the fibril ends (the elongation phase). In many amyloid systems, this mechanism is complicated by the early formation of

Ronald Wetzel was born in Hanover, PA, in 1946. He obtained a B.S. in Chemistry from Drexel University in 1969 and a Ph.D. in physical organic chemistry from the University of California, Berkeley, in 1973, after which came postdoctoral training at the Max Planck Institute for Experimental Medicine and at Yale University. He has served as a senior scientist at Genentech and as a senior research fellow at SmithKline Beecham and is now Professor in the Graduate School of Medicine at the University of Tennessee. His main scientific interest for 25 years has been protein misfolding and aggregation.

* Current address: Department of Structural Biology, University of Pittsburgh School of Medicine, 3501 Fifth Avenue, Pittsburgh, PA 15260.

10.1021/ar050069h CCC: $33.50
Published on Web 07/22/2006

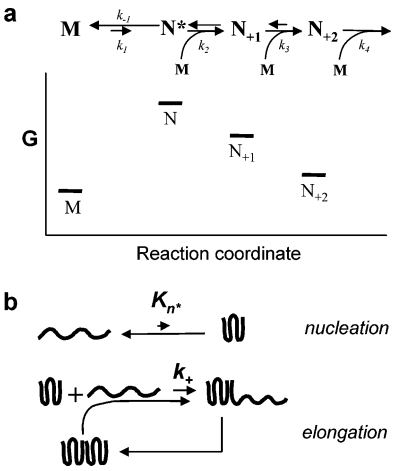

FIGURE 1. The thermodynamic model of nucleated growth polymerization: (a) a general model showing formation of the nucleus N* as a rapid, reversible, unfavorable equilibrium, and how elongation of N* by monomers M to form early aggregates N_{+1}, N_{+2}, etc., leads to stabilization of the system; (b) mechanism of nucleation of polyglutamine aggregation showing the nucleus as a folded monomer and elongation as a series of bimolecular addition steps with unfolded monomer. Reprinted with permission from ref 19. Copyright 2002 National Academy of Sciences, U.S.A.

a variety of noncovalent oligomeric structures,[14] but simple polyglutamine peptides do not appear to form such oligomers under native conditions, allowing relatively straightforward study of both kinetic phases of amyloid growth.

Nucleation. The thermodynamic model of aggregation nucleation (Figure 1a) considers the nucleus to be the least stable identifiable species on the aggregation pathway and to exist in a pre-equilibrium in rapid interchange with ground-state monomers, such that the nucleation rate contains contributions from both the equilibrium constant for nucleus formation and the rate constant for nucleus elongation.[13] In this model, the nucleus, once formed, can either decay back to the ground state or proceed by a series of elongation steps, each of which further stabilizes the system. According to the mathematical relationship, eq 1, based on this model, Δ (the amount of monomer converted to aggregate at time t) depends on c, the concentration of monomer; n^*, the critical nucleus or number of monomers that come together to form the nucleus; K_{n^*}, the nucleation equilibrium constant describing the pre-equilibrium between the bulk monomer pool and the nucleus; and k_+, the second-order elongation rate constant, which for simplicity is assumed to be identical for reactions of both the nucleus and early aggregates.

$$\Delta = {}^1/_2 k_+{}^2 K_{n^*} c^{(n^*+2)} t^2 \qquad (1)$$

Huntington's disease and other expanded CAG repeat diseases are triggered by the genetic expansion of a polyglutamine sequence in a protein to a repeat length typically of about 40 glutamines or higher. Aggregation of polyglutamine is implicated in the disease mechanism by a number of observations,[12,15] including the fact that the dependence of disease risk and disease aggressiveness

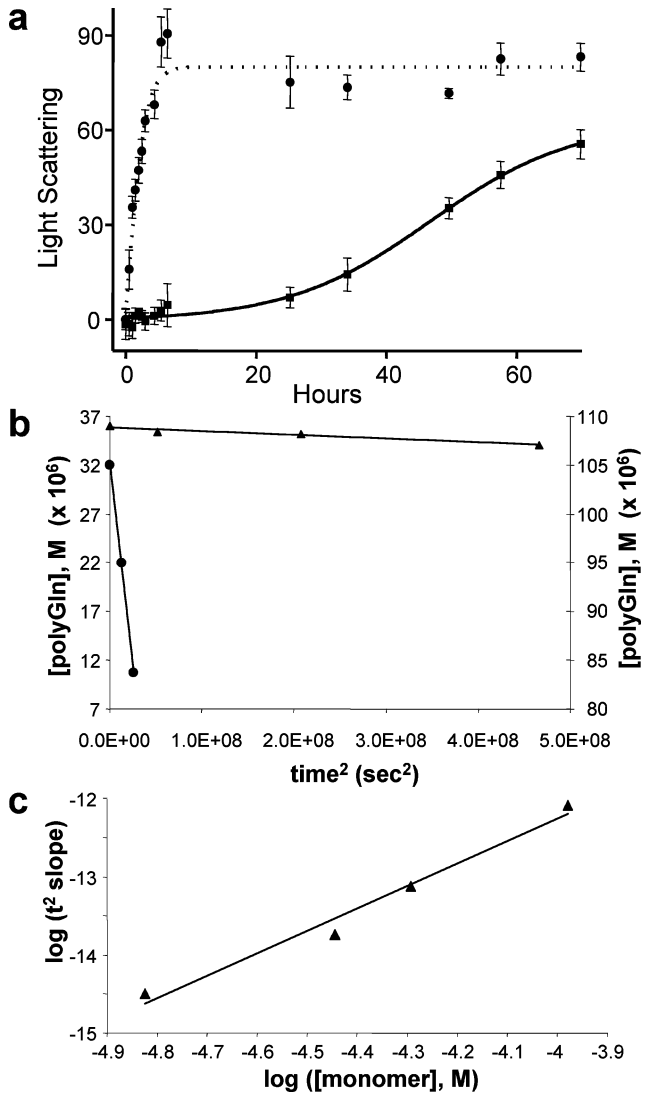

FIGURE 2. Aspects of polyglutamine aggregation kinetics: (a) aggregation of a disaggregated solution of polyglutamine with (●) and without (■) seeding by previously made polyglutamine aggregate (Reprinted from ref 39, copyright 2001, with permission from Elsevier); (b) t^2 plot of the early spontaneous aggregation kinetics for a polyglutamine peptide (▲, left y-axis; ●, right y-axis);[20] (c) log−log plot for the determination of the critical nucleus N* for polyglutamine aggregation. Parts b and c reprinted with permission from ref 20. Copyright 2005 National Academy of Sciences, U.S.A.

on the repeat length of the polyglutamine sequence[16] is mirrored by the repeat length dependence of polyglutamine aggregation.[12]

Preliminary studies of the aggregation of rigorously disaggregated[17] simple polyglutamine peptides suggested a nucleated growth mechanism. Thus, the reaction exhibits a lag phase that can be aborted if the reaction is provided a seed of preformed aggregate (Figure 2a), two features consistent with slow nucleus formation.[18] Analyses based on eq 1 provided further confirmation of a nucleated growth polymerization pathway, as well as key reaction parameters.[19] Thus, the early stages of spontaneous aggregation can be fit to a linear t^2 plot (Figure 2b), and the logs of the slopes of these plots increased linearly with the log of the peptide concentrations used (Figure

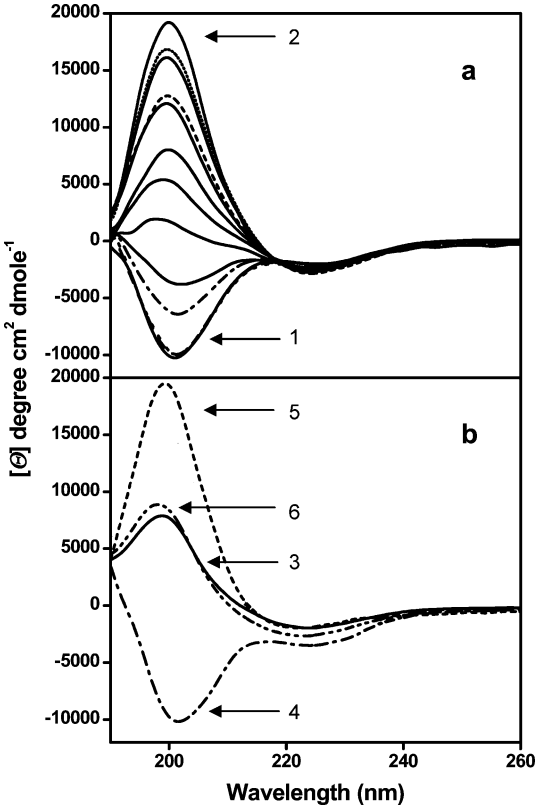

FIGURE 3. Acquisition of β-structure concerted with aggregation. Circular dichroism spectra of the aggregation of a Q_{42} peptide in Tris·HCl, pH 7: (a) time course of aggregation reaction from $t = 0$ (curve 1) to $t = 217$ h (curve 2) showing a two-state random coil to β-sheet transition; (b) an aliquot of the 90 h time point (curve 3) from panel a was subjected to ultracentrifugation, and the supernatant (curve 4) and resuspended pellet (curve 5) were recorded. The sum of curves 4 and 5 (curve 6) matches well with curve 3. Adapted with permission from ref 19. Copyright 2002 National Academy of Sciences, U.S.A.

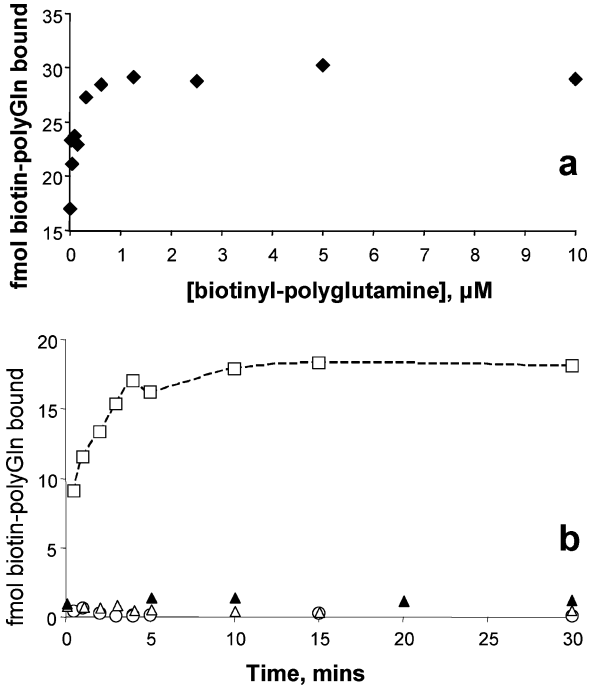

FIGURE 4. Characterization of polyglutamine aggregation reactions: (a) concentration dependence of the addition of a biotin-labeled polyglutamine monomer to an amyloid-like polyglutamine aggregate under conditions disfavoring elongation; (b) time dependence of the binding of biotinyl-polyglutamine to the polyglutamine aggregate, using incubation of each time point with excess unlabeled Q_{30} to stimulate multiple rounds of addition and thus inhibit label dissociation (□), control in which unlabeled Q_{30} was left out (○), experiment adding biotin-linked Aβ(1−40) to the Q_{47} aggregate (▲), and experiment incubating a biotin-linked, elongation-incompetent proline mutant of polyglutamine[40] to the Q_{47} aggregate (△). Reprinted with permission from ref 20. Copyright 2005 National Academy of Sciences, U.S.A.

2c). Surprisingly, the slope of the log−log plot, which is equal to $n^* + 2$, yielded a value for the critical nucleus of one; that is, in contrast to the classical view of the nucleus as an oligomeric structure, the nucleus for polyglutamine aggregation appears to be an alternative folded state of the monomer.[19] Circular dichroism analysis suggests that β-sheet formation and aggregate formation may be concerted processes: First, the random coil to β-sheet transition observed during the aggregation reaction (Figure 3a) displays an isosbestic point and parallels reaction progress monitored by other measures of aggregation.[19] Second, CD spectra of the supernatant and pellet fractions of an aggregation reaction midpoint are identical to those of starting material and product and do not suggest the presence of a significant amount of β-sheet-rich monomers or small oligomers during reaction (Figure 3b). Based on the above data, we proposed a model for the spontaneous aggregation process in which the nucleation event is depicted as a highly unfavorable protein folding reaction and the elongation step to involve encounters between nuclei/aggregates and ground state, unstructured molecules of polyglutamine (Figure 1b).[19]

Further analysis suggests that the increase in spontaneous polyglutamine aggregation rate with repeat length derives mainly from increases in K_{n^*}.[19] This suggests a mechanism by which polyglutamine repeat length, through its control over the energetics of nucleus formation, provides a driving force for aggregation in the cell, which, modulated as it must be by other cellular factors, ultimately determines the aggressiveness of disease.

To further dissect the components of the nucleation process and provide an estimate of K_{n^*}, it is necessary to independently determine realistic values for the second-order elongation rate constants. As described in the next section, fibril elongation in the most simple case results in fibril growth without an increase in the molar concentration of fibrils, such that the reaction is described by pseudo-first-order kinetics. Polyglutamine fibril elongation, in fact, follows such kinetics, and it is straightforward to determine a pseudo-first-order rate constant. Without a knowledge of the molar concentration of fibrils (or, in other words, the effective molecular weight of a fibril preparation), however, it is not possible to determine the underlying second-order rate constant for elongation, which is the parameter required by eq 1. To provide such estimates, we developed a method for titration of the

growth sites in a suspension of fibrils, using a biotinylated form of monomeric polyglutamine.[20] As expected, growth sites quantified by this procedure are saturable (Figure 4a), are increased if fibrils are sonicated, shed the tagged polyglutamine if subsequent rounds of elongation do not occur (Figure 4b), and do not occur with monomer−fibril combinations known to exhibit negligible seeded growth (Figure 4b). Using molar fibril concentrations determined by this method, we were able to calculate an estimate for K_{n^*} for a Q_{47} sequence of about 10^9. This value brings home the incredibly low concentration of nuclei present at any one time during nucleated growth, the health consequences of which nonetheless loom large.

Elongation. Because elongation proceeds equally well from endogenous nuclei and exogenous seeds, it is possible to study the elongation process in isolation by studying seeded fibril growth. This is particularly useful when determining parameters required for dissecting nucleated growth kinetics, as described above, and also in studying fibril formation reactions where the nucleation step is more obscure or complex, such as in the case of fibril formation by the Alzheimer's plaque peptide Aβ.

A variety of methods are available for studying elongation reactions. In suspension phase, aggregation can be followed directly by estimating aggregate mass using the ability of aggregates to bind thioflavin T and induce fluorescence spectrum changes or indirectly by using a sedimentation assay to determine the amount of monomer left unpolymerized at different times.[17] Figure 5a shows that both methods produce essentially the same rates, although some thought must go into analysis of reactions that do not go to completion.[21] Solid-phase assays have also been described. Microtiter plate assays, in which seeds are immobilized onto plastic and the incorporation of monomer into fibrils over time is monitored with radiolabeled [22] or biotinylated [23] peptide (Figure 5b), are particularly useful tools for screening for small molecule modulators of aggregation.[24] Fibril elongation can also be observed by surface plasmon resonance (SPR).[25] Global analysis of SPR association and dissociation curves at different monomer concentrations allowed derivation of a set of microscopic rate constants describing individual steps of the elongation process.[25] Both the SPR and microplate assays show elongation to be a multistep process featuring relatively rapid addition of a fresh monomer to the growth site on the fibril, followed by one or more relatively slow steps presumably associated with folding of the newly added monomer into an amyloid conformation, in the process generating a fresh elongation site.[22,25]

Seeded fibril elongation can be used to explore amyloid fibril structure, by inquiring into the compatibility of one amyloidogenic peptide with another in a "cross-seeding" reaction. That is, each rung of the amyloid ladder contains a repeat folding unit that can be thought of as a microdomain that must make snug noncovalent contacts with its neighbors to propagate the fibril; the efficiency of cross-seeding should be a measure of this snugness of fit for the incoming monomer. In a study using both the microplate assay and solution phase assays, we found that when two amyloidogenic peptides differ significantly in amino acid sequence, the ability of a fibril of one to stimulate elongation by another is, while measurable, relatively inefficient (Figure 5b). However, fibrils of single point mutants of Aβ(1−40) can be very efficient seeds for elongation of wild-type Aβ(1−40), especially if the mutations are outside the H-bonded, β-sheet amyloid core.[23] In the future, the most accurate comparisons of elongation rate constants in such cross-seeding experiments will require normalization of the data with respect to the number of growth sites per weight of fibril, as determined, for example, by the growing ends titration[20] described above.

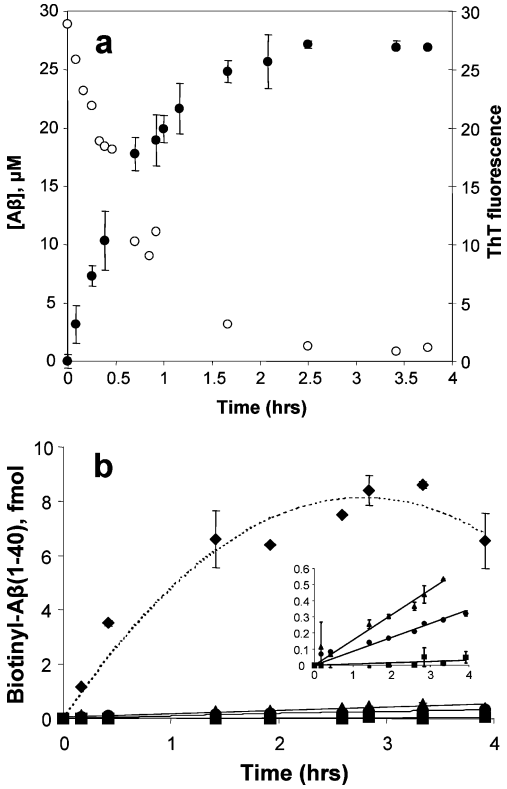

FIGURE 5. Seeded elongation of Aβ(1−40): (a) in suspension phase monitored by ThT fluorescence (●) and by an HPLC-based sedimentation assay (○) (Reprinted with permission from ref 21. Copyright 2005 American Chemical Society); (b) in a microtiter plate assay using fluorescence to observe the deposition of monomeric biotinyl-Aβ(1−40) in response to plastic-immobilized aggregates of Aβ(1−40) amyloid fibrils (◆), amyloid-like polyglutamine aggregates (▲), islet amyloid polypeptide amyloid fibrils (●), and collagen (■). Inset shows the early time points with an expanded *y*-scale. Reprinted from ref 23. Copyright 2004 ASBMB.

Thermodynamics of Amyloid Formation

Noncovalent off-pathway aggregation is traditionally thought of as being an essentially irreversible reaction leading to highly insoluble precipitates that can only be rescued, if at all, by a denaturation/renaturation cycle. This impression, often based on observations of essentially nil aggregate solubility, led to the classical view of the nonnative aggregate as an irregular tangle of polypeptide chains intertwined in a hopeless Gordian knot. It was

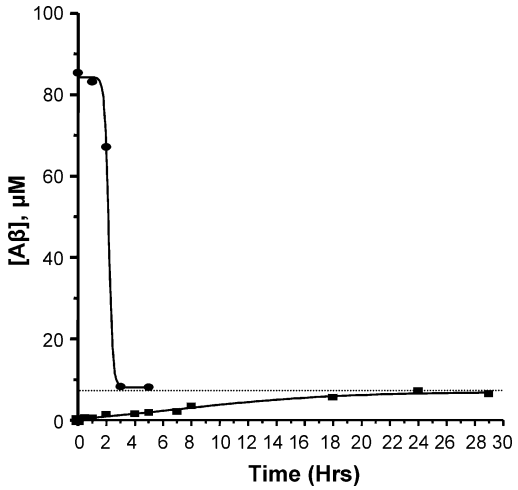

FIGURE 6. Reversibility of amyloid fibril growth of the S26P point mutant of Aβ(1−40) monitored by a HPLC sedimentation assay. Seeded elongation of fibrils proceeds to a plateau value for remaining soluble Aβ (●). Dilution of the final amyloid fibril product leads to dissociation of monomer to a plateau position equivalent to that of the forward reaction (■). Reprinted with permission from ref 21. Copyright 2005 American Chemical Society.

particularly surprising, therefore, to realize that at least some amyloid fibrils grow to a reversible equilibrium position exhibiting a characteristic equilibrium constant and associated free energy of elongation. Previous studies demonstrated such an equilibrium in Aβ(1−40) fibril formation leading to a residual concentration of monomer characteristic of the reaction, the critical concentration or C_r.[26] More recently, the robustness of this equilibrium position was examined for Aβ(1−40) and found to meet all criteria for a reversible reaction lodged at a thermodynamic endpoint,[21] including the ability of resuspended fibrils to dissociate to an identical C_r value (Figure 6). Since, at equilibrium, the molar concentration of fibrils on either side of the elongation equation are identical, the equilibrium constant in the growth direction reduces to 1/[monomer], which, at equilibrium, is $1/C_r$. The ability to determine the equilibrium constant for fibril elongation allows calculation of the ΔG associated with that process.[21,27,28] Based on these considerations, we realized that comparison of the amyloid growth C_r values for two peptides differing in sequence at one position should allow us to determine a $\Delta\Delta G$ for elongation.[21,28] Measurement and manipulation of C_r values and derived energetic parameters has allowed a number of important insights into Aβ(1−40) amyloid fibril structure and energetics, as discussed in the following sections.

$\Delta\Delta G$ Values Primarily Sensing Fibril Packing Effects. Analysis of mutational effects on free energies of elongation is perhaps especially informative when done on a series of related mutants, such as in alanine scanning or proline scanning. Thus, fibril growth of a series of single proline mutants of Aβ(1−40) was examined.[28] This study was designed to uncover sequence positions in Aβ(1−40) that are sensitive to proline replacement,[29] since highly sensitive ones are likely to be involved in the H-bonded β-sheet amyloid core. Every proline mutant examined was able to make fibrils and arrive at an equilibrium position, although the C_r for some proline mutants is hundreds of times higher than wild-type C_r. Derivation of the related ΔG values for elongation allowed construction of a $\Delta\Delta G$ bar graph summarizing the mutational effects on stability (Figure 7a). The data show that some proline replacements have little impact on fibril structure, while others (such as those at positions 19 and 20) are significantly destabilizing. Relatively insensitive sites seem to map out a punctuated sequence in which residues from 1 to 14, 22, 23, 29, 30, and 37−40 are not greatly involved in the formation of the amyloid core. Interestingly, combining four of these null mutations into a tetra-proline mutant gave an Aβ sequence that makes amyloid fibrils about as well as wild type despite its 10% proline content;[28] in contrast, a double proline mutant at the sensitive positions 19 and 32 produced an exceedingly destabilized fibril.[24] These data were used in combination with a threading approach to produce a preliminary working model of an Aβ(1−40) amyloid fibril.[30] This model agrees in some respects with and differs in other respects from models of Aβ(1−40) amyloid fibrils (formed under different growth conditions; see below) derived from solid-state NMR studies.[31] Residues 15−21 and 31−36 are strongly implicated to be in β-sheet structure by the proline scanning results, in agreement with solid-state NMR results and other studies.

One surprising aspect of this study was the finding that fibril stability does not necessarily go hand-in-hand with the number of backbone H-bonds in the β-sheet network. Using hydrogen−deuterium exchange to determine the number of highly protected, presumably H-bonded, backbone amide hydrogens in the fibril, we found that in some cases mutant fibrils that are destabilized with respect to wild-type fibrils actually contain more protected hydrogens.[28] This shows that amyloid fibril stability is determined by a balance of a variety of molecular forces, in analogy to globular protein stability.[28]

More recently, an alanine scan of Aβ(1−40) was reported.[32] This allowed assessment of the contribution of each wild-type side chain to fibril structure. The results (Figure 7b) are largely consistent with models showing the 15−21 and 31−36 segments to be the major hydrophobic packing elements. The alanine scan results at some positions allowed us to directly compare the effects of particular amino acid substitutions in packed, parallel β-sheet in an amyloid fibril with similar data for the small, globular protein Gβ1.[33] Table 1 shows a comparison of $\Delta\Delta G$ values for amino acid to alanine mutations for several different amino acids. Considering the widely different methods used for acquiring the data, the widely different structural motifs of the proteins, and the different unique environments for each amino acid side chain in the amyloid fibril and globular protein being compared, we think the degree of agreement of the results is remarkable. The agreement suggests that ΔG values derived from amyloid C_r values give similar information to extrapolation of denaturant unfolding curves for globular proteins and provide additional evidence that amyloid

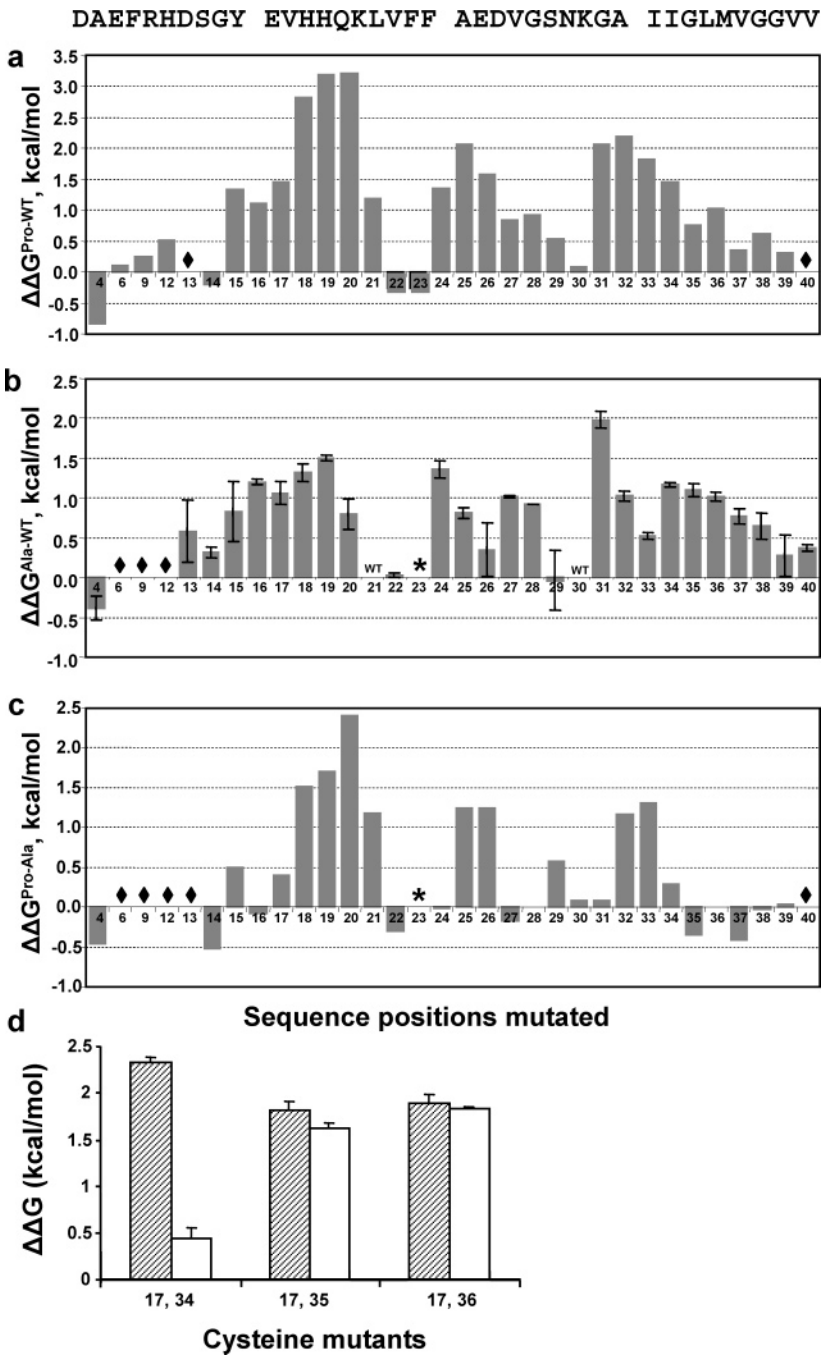

FIGURE 7. Thermodynamic analysis of Aβ(1−40) elongation reaction in response to mutations. The amino acid sequence of Aβ(1−40) is shown at the top. For any mutation, a positive $\Delta\Delta G$ is associated with destabilization with respect to the ΔG for wild type, which is set at zero: (a) $\Delta G^{Pro} - \Delta G^{WT}$ for single proline mutants of Aβ(1−40) (Adapted from ref 28, Copyright 2004, with permission from Elsevier); (b) $\Delta G^{Ala} - \Delta G^{WT}$ for single alanine mutants;[32] (c) $\Delta G^{Pro} - \Delta G^{Ala}$ obtained by subtraction of the data in parts a and b (Parts b and c adapted from ref 32, Copyright 2006, with permission from Elsevier); (d) $\Delta G^{mutant} - \Delta G^{WT}$ for a single series of oxidized (open bars) and reduced (hatched bars) double cysteine mutants (Reprinted with permission from ref 35. Copyright 2004 American Chemical Society).

fibrils are stabilized by the same types of interactions as those found in globular proteins.

Alanine scan data was also used to adjust the previously determined proline scan data to generate what is effectively a series of proline−alanine $\Delta\Delta G$ values. By making the assumption that the alanine side chain is a reasonably good approximation of the hydrophobicity of the proline side chain, these proline−alanine $\Delta\Delta G$ values can be thought of as showing for each residue position in the fibril how deeply fibril stability is affected by the proline replacement, without any large overlays from hydrophobicity differences. The results (Figure 7c) resemble those of the proline scan (Figure 7a) while at the same time exhibiting a number of differences, including some amino acid positions where the difference between alanine and proline is negligible, even though the residue yields a significant proline−wild type $\Delta\Delta G$ (Figure 7a). One surprising feature of these studies is that proline

Table 1. Alanine Destabilization of Amyloid Fibrils and Globular Proteins[a]

	$\Delta\Delta G_{(\text{alanine}-\text{residue})}$, kcal/mol						
	G(β1) position[b]	Aβ(1−40) amyloid fibril position[b]					
mutation	6 + 53	18	19	20	31	32	36
Val→Ala	1.25	1.3					1.0
Phe→Ala	1.5		1.5	0.8			
Ile→Ala	1.65				2.0	1.0	

[a] The free energy effects of alanine mutations at different sequence positions on the protein folding equilibria of the G(β1) domain and Aβ(1−40) fibrils are listed. Each column contains data for an amino acid to alanine mutation at a particular position (Aβ fibrils) or positions (G(β1)). [b] G(β1) data from ref 33. Aβ(1−40) data from ref 32. Values shown are on a per-residue basis, so the G(β1) data for the effect of a double replacement[33] is divided by two.

replacements at some positions widely regarded as being in β-sheet structure in the fibril nonetheless seem energetically neutral (for example, residues 31, 34, 35, and 36). This may be due to compensating structural adjustments, such as the acquisition of additional H-bonds mentioned above.

Thermodynamic analysis has also been used in a number of ways to look at cysteine mutations of Aβ(1−40). In one series of experiments, single cysteine mutants were derivatized with either iodoacetic acid or iodomethane to produce negatively charged or neutral hydrophobic chemical mutants, and the free energies of elongation for each mutant were determined as described above.[34] The data largely agrees with the results of the alanine scan in indicating which parts of the sequence are likely to be in buried or exposed structure in the fibril. In another series of experiments, several disulfide cross-linked monomeric Aβ(1−40) mutants were produced and grown into fibrils, and the C_r's were determined. The $\Delta\Delta G$ values for the different mutants in their reduced and oxidized states (Figure 7d) indicated which amino acid side chains are likely to be in contact within the packed structure of the wild-type fibril. These results were in very good agreement with independent cross-linking experiments that implicate residues 17 and 34 in an intramolecular packing interaction within Aβ in the fibril.[35]

Despite a number of important caveats to the interpretation of C_r-derived $\Delta\Delta G$ values for amyloid elongation (see below), these measurements appear to give quality data that are in very good agreement with similar data derived from globular protein studies and that can be used to help address issues of amyloid structure, as well as the structural dynamics within the amyloid fibril.

$\Delta\Delta G$ Values Primarily Sensing Monomer Conformational Effects. The ΔG for a reaction depends on the difference in free energy between the starting and ending states. Therefore, a particular $\Delta\Delta G$ can be obtained in numerous ways, by different combinations of mutational effects on the free energy of the starting and ending states (Figure 8). The interesting trends seen in the mutational scans discussed above appear to derive mostly from effects on the fibril state.[32] However, mutations can sometimes have great impact through their action on the free energy of the native, monomeric state of a peptide.

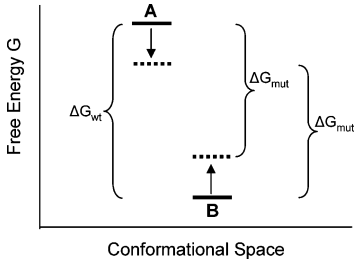

FIGURE 8. Schematic energy landscape for monomer−fibril transformations. This figure illustrates two ways that mutation could lead to an equivalent decrease in the ΔG for fibril formation, either by stabilization of the monomer (A) or by destabilization of the aggregate (B). Monomer stabilization can occur either via stabilization of a single, highly populated monomer conformation or by a shift within the monomer ensemble (i.e., due to higher stability) to greater occupancy by an aggregation-incompetent set of conformations.

An example is the effect of an oligoproline sequence appended to the C-terminus of a polyglutamine sequence, as occurs in the protein huntingtin.[36] The attachment of a P_{10} segment onto the C-terminus of a Q_{40} sequence, for example, slows aggregation kinetics while greatly increasing (by 30-fold or more) the C_r of the aggregation reaction (Figure 9a). Interestingly, the effect is lost if the P_{10} sequence is attached to the C-terminus through a side chain covalent attachment or appended via a peptide bond to the N-terminus, rather than the C-terminus, of polyglutamine (Figure 9a). The effect appears to be realized on the solution phase peptide, rather than on the aggregate.[36]

The most likely explanation for this effect is that the P_{10} sequence effectively stabilizes the monomeric state of the peptide, by reducing the percentage of monomeric peptide in an aggregation competent conformation (Figure 8).[36] This is consistent with CD studies showing that the C-terminal P_{10} sequence appears to favor the formation/stability of alternative polyglutamine conformations.[36] Further work is required to dissect the normal distribution of folded states of Q_{40} in the monomer in solution and how this distribution is affected by the appended P_{10} sequence. Interestingly, placement of a P_{10} sequence on the C-terminus of Aβ(1−40) elevates the C_r of this peptide's amyloid formation reaction to a similar extent.[36]

Extrinsic (Non-Amino Acid Sequence) Effects on Fibril Formation Kinetics and Thermodynamics. Besides adjacent sequence elements as discussed above, environmental factors can also greatly affect aggregation kinetics and thermodynamics. Figure 9b shows the affect of the molecular crowding agent poly(ethylene glycol) on polyglutamine aggregation. While molecular crowding agents have previously been shown to affect the kinetics of amyloid formation,[37] the result in Figure 9 suggests that crowding agents can also stabilize the monomer−aggregate equilibrium, making it possible for smaller concentrations of a peptide to support aggregation. This may be especially important in helping to explain why amyloid growth occurs in vivo despite relatively high C_r values determined in vitro.[36]

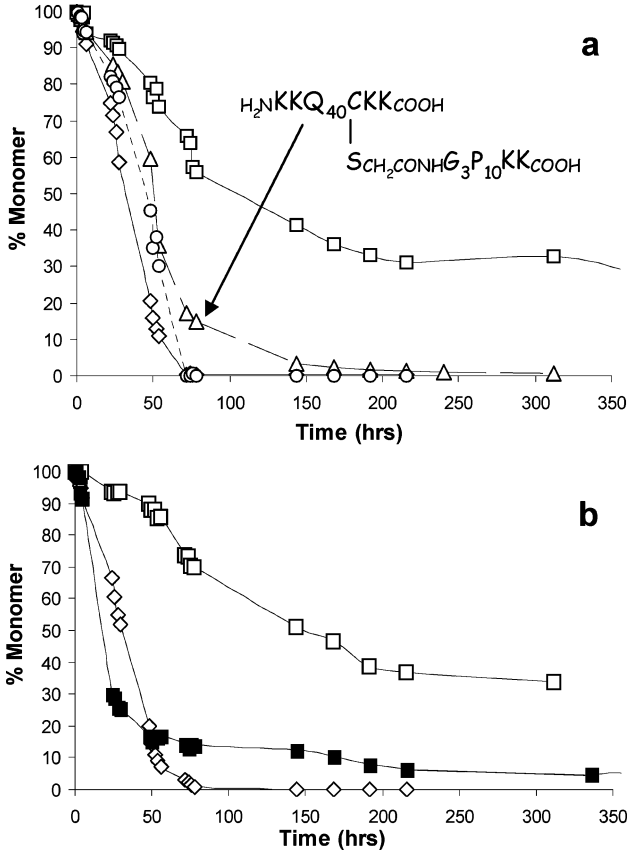

FIGURE 9. Modulation of polyglutamine aggregation kinetics and thermodynamics: (a) context-dependent effects of an oligoproline sequence on polyglutamine aggregation—shown are aggregation time courses for a simple polyglutamine sequence (◇), polyglutamine with C-terminal P_{10} (□), polyglutamine with N-terminal P_{10} (○), and polyglutamine with P_{10} connected to a side chain as shown in the insert (△); (b) cosolute effects on polyglutamine aggregation—shown are aggregation of Q_{40} peptide in PBS (◇), $Q_{40}P_{10}$ in PBS (□), and $Q_{40}P_{10}$ in PBS plus 150 mg/mL poly(ethylene glycol) (■). Reprinted from ref 36, Copyright 2006, with permission from Elsevier.

Caveats and Limitations to the Use of ΔΔ*G*'s for Amyloid Fibril Elongation. As is the case for mutational analysis of globular protein folding stability, the derivation of thermodynamic values for fibril elongation in response to mutation is grounded in a number of assumptions that may not always be valid. It is important to keep in mind some caveats and qualifications,[32] including the following:

(a) As discussed above, mutations can affect both the folded (fibril) and unfolded (monomer) states.

(b) One peptide sequence can form multiple conformations of amyloid fibrils.[38] Given this, it is theoretically possible that a mutation may play a role in directing which conformation the peptide grows into. However, preliminary studies suggest that growth conditions play a greater role in directing fibril conformation than do point mutations (R. Kodali and R. Wetzel, unpublished). Seeding fibril growth of mutant monomers by using a common conformation, for example, of wild-type fibrils grown in a certain way may help put mutant fibrils on a common conformational ground.[32]

(c) Amyloid fibrils exhibit a significant structural plasticity, apparently to a greater extent than do typical globular proteins. Evidence for this includes nonadditivity of distal mutational effects,[32] distal formation of new H-bonds in response to point mutation,[28] and resiliency of fibril formation in response to forced, major structural changes.[35] One implication of this caveat is that the full local energetic effect of a mutation may be underestimated in the measured ΔΔ*G* because of compensating changes elsewhere in the fibril structure. This obviously places limitations of the use of such analyses as a pure structure elucidation tool. At the same time, scanning mutagenesis with ΔΔ*G* analysis, conducted in the context of structural information, can clearly provide insights into how amyloid fibrils are put together in a way that either technique in isolation cannot.

Conclusions

It remains to be seen how generally applicable some of the analyses described in this Account will be for studies on other amyloids and other aggregates. Detailed analysis of nucleation kinetics will be more complex and possibly beyond the reach of the mathematical approach described here in systems in which elongation-incompetent oligomers and protofibrils accumulate in the early phases of spontaneous amyloid growth. Thermodynamic analysis of the elongation reaction of amyloid fibrils is relatively simple if the fibril exhibits an easily measured C_r, and much more challenging if it does not. Nonetheless, the existence of just one or two amenable systems should allow us to probe further into general features of the structures and assembly mechanisms of amyloid fibrils and other aggregates.

References

(1) Mitraki, A.; Fane, B.; Haase-Pettingell, C.; Sturtevant, J.; King, J. Global suppression of protein folding defects and inclusion body formation. *Science* **1991**, *253*, 54−58.
(2) Meriin, A. B.; Sherman, M. Y. Role of molecular chaperones in neurodegenerative disorders. *Int. J. Hyperthermia* **2005**, *21*, 403−419.
(3) Schein, C. H. Production of soluble recombinant proteins in bacteria. *Biotechnology* **1989**, *7*, 1141−1149.
(4) De Bernardez Clark, E.; Schwarz, E.; Rudolph, R. Inhibition of aggregation side reactions during in vitro protein folding. *Methods Enzymol.* **1999**, *309*, 217−236.
(5) Martin, J. B. Molecular basis of the neurodegenerative disorders. *N. Engl. J. Med.* **1999**, *340*, 1970−1980 [published erratum appears in *N. Engl. J. Med.* **1999**, *341* (18), 1407].
(6) Merlini, G.; Bellotti, V. Molecular mechanisms of amyloidosis. *N. Engl. J. Med.* **2003**, *349*, 583−596.
(7) Chapman, M. R.; Robinson, L. S.; Pinkner, J. S.; Roth, R.; Heuser, J.; Hammar, M.; Normark, S.; Hultgren, S. J. Role of *Escherichia coli* curli operons in directing amyloid fiber formation. *Science* **2002**, *295*, 851−855.
(8) Fink, A. L. Protein aggregation: folding aggregates, inclusion bodies and amyloid. *Folding Des.* **1998**, *3*, R9−23.
(9) Wetzel, R. Mutations and off-pathway aggregation. *Trends Biotechnol.* **1994**, *12*, 193−198.
(10) Hammarstrom, P.; Wiseman, R. L.; Powers, E. T.; Kelly, J. W. Prevention of transthyretin amyloid disease by changing protein misfolding energetics. *Science* **2003**, *299*, 713−716.
(11) Selkoe, D. J. The origins of Alzheimer disease: a is for amyloid. [editorial; comment] *JAMA, J. Am. Med. Assoc.* **2000**, *283*, 1615−1617.
(12) Bates, G. P.; Benn, C. In *Huntington's Disease*; Bates, G. P., Harper, P. S., Jones, L., Eds.; Oxford University Press: Oxford, U.K., 2002; pp 429−472.
(13) Ferrone, F. Analysis of protein aggregation kinetics. *Methods Enzymol.* **1999**, *309*, 256−274.

(14) Harper, J. D.; Lieber, C. M.; Lansbury, P. T., Jr. Atomic force microscopic imaging of seeded fibril formation and fibril branching by the Alzheimer's disease amyloid-beta protein. *Chem. Biol.* **1997**, *4*, 951−959.
(15) Wetzel, R. In *Genetic instabilities and neurological diseases*; 2nd ed.; Wells, R., Ashizawa, T., Eds.; Elsevier: San Diego, CA, 2006; in press.
(16) Scherzinger, E.; Sittler, A.; Schweiger, K.; Heiser, V.; Lurz, R.; Hasenbank, R.; Bates, G. P.; Lehrach, H.; Wanker, E. E. Self-assembly of polyglutamine-containing huntingtin fragments into amyloid-like fibrils: implications for Huntington's disease pathology. *Proc. Natl. Acad. Sci. U.S.A.* **1999**, *96*, 4604−4609.
(17) O'Nuallain, B.; Thakur, A. K.; Williams, A. D.; Bhattacharyya, A. M.; Chen, S.; Thiagarajan. G.; Wetzel, R. Kinetics and thermodynamics of amyloid assembly using an HPLC-based sedimentation assay. *Methods Enzymol.* **2006**, in press.
(18) Chen, S.; Berthelier, V.; Hamilton, J. B.; O'Nuallain, B.; Wetzel, R. Amyloid-like features of polyglutamine aggregates and their assembly kinetics. *Biochemistry* **2002**, *41*, 7391−7399.
(19) Chen, S.; Ferrone, F.; Wetzel, R. Huntington's Disease age-of-onset linked to polyglutamine aggregation nucleation. *Proc. Natl. Acad. Sci. U.S.A.* **2002**, *99*, 11884−11889.
(20) Bhattacharyya, A. M.; Thakur, A.; Wetzel, R. Polyglutamine aggregation nucleation: thermodynamics of a highly unfavorable protein folding reaction. *Proc. Natl. Acad. Sci. U.S.A.* **2005**, *102*, 15400−15405.
(21) O'Nuallain, B.; Shivaprasad, S.; Kheterpal, I.; Wetzel, R. Thermodynamics of abeta(1−40) amyloid fibril elongation. *Biochemistry* **2005**, *44*, 12709−12718.
(22) Esler, W. P.; Stimson, E. R.; Jennings, J. M.; Vinters, H. V.; Ghilardi, J. R.; Lee, J. P.; Mantyh, P. W.; Maggio, J. E. Alzheimer's disease amyloid propagation by a template-dependent dock-lock mechanism. *Biochemistry* **2000**, *39*, 6288−6295.
(23) O'Nuallain, B.; Williams, A. D.; Westermark, P.; Wetzel, R. Seeding specificity in amyloid growth induced by heterologous fibrils. *J. Biol. Chem.* **2004**, *279*, 17490−17499.
(24) Williams, A. D.; Sega, M.; Chen, M.; Kheterpal, I.; Geva, M.; Berthelier, V.; Kaleta, D. T.; Cook, K. D.; Wetzel, R. Structural properties of Aβ protofibrils stabilized by a small molecule. *Proc. Natl. Acad. Sci. U.S.A.* **2005**, *102*, 7115−7120.
(25) Cannon, M. J.; Williams, A.; Wetzel, R.; Myszka, D. G. Kinetic Analysis of Aβ Fibril Elongation. *Anal. Biochem.* **2004**, *328*, 67−75.
(26) Jarrett, J. T.; Costa, P. R.; Griffin, R. G.; Lansbury, P. T., Jr. Models of the b protein C-terminus: differences in amyloid structure may lead to segregation of "long" and "short" fibrils. *J. Am. Chem. Soc.* **1994**, *116*, 9741−9742.
(27) Hasegawa, K.; Ono, K.; Yamada, M.; Naiki, H. Kinetic modeling and determination of reaction constants of Alzheimer's beta-amyloid fibril extension and dissociation using surface plasmon resonance. *Biochemistry* **2002**, *41*, 13489−13498.
(28) Williams, A. D.; Portelius, E.; Kheterpal, I.; Guo, J. T.; Cook, K. D.; Xu, Y.; Wetzel, R. Mapping abeta amyloid fibril secondary structure using scanning proline mutagenesis. *J. Mol. Biol.* **2004**, *335*, 833−842.
(29) Wood, S. J.; Wetzel, R.; Martin, J. D.; Hurle, M. R. Prolines and amyloidogenicity in fragments of the Alzheimer's peptide β/A4. *Biochemistry* **1995**, *34*, 724−730.
(30) Guo, J.-T.; Wetzel, R.; Xu, Y. Molecular modeling of the core of Aβ amyloid fibrils. *Proteins* **2004**, *57*, 357−364.
(31) Petkova, A. T.; Yau, W. M.; Tycko, R. Experimental Constraints on Quaternary Structure in Alzheimer's beta-Amyloid Fibrils. *Biochemistry* **2006**, *45*, 498−512.
(32) Williams, A. D.; Shivaprasad, S.; Wetzel, R. Alanine scanning mutagenesis of Aβ(1−40) amyloid fibril stability. *J. Mol. Biol.* **2006**, *357*, 1283−1294.
(33) Merkel, J. S.; Sturtevant, J. M.; Regan, L. Side chain interactions in parallel beta sheets: the energetics of cross-strand pairings. *Struct. Folding Des.* **1999**, *7*, 1333−1343.
(34) Shivaprasad, S.; Wetzel, R. Scanning cysteine mutagenesis analysis of Aβ(1−40) amyloid fibrils. *J. Biol. Chem.* **2006**, *281*, 993−1000.
(35) Shivaprasad, S.; Wetzel, R. An intersheet packing interaction in Aβ fibrils mapped by disulfide cross-linking. *Biochemistry* **2004**, *43*, 15310−15317.
(36) Bhattacharyya, A. M.; Thakur, A. K.; Hermann, V. M.; Thiagarajan, G.; Williams, A. D.; Chellgren, B. W.; Creamer, T. P.; Wetzel, R. Oligoproline effects on polyglutamine conformation and aggregation. *J. Mol. Biol.* **2006**, *355*, 524−535.
(37) Shtilerman, M. D.; Ding, T. T.; Lansbury, P. T., Jr. Molecular crowding accelerates fibrillization of alpha-synuclein: could an increase in the cytoplasmic protein concentration induce Parkinson's disease? *Biochemistry* **2002**, *41*, 3855−3860.
(38) Petkova, A. T.; Leapman, R. D.; Guo, Z.; Yau, W. M.; Mattson, M. P.; Tycko, R. Self-propagating, molecular-level polymorphism in Alzheimer's β-amyloid fibrils. *Science* **2005**, *307*, 262−265.
(39) Chen, S.; Berthelier, V.; Yang, W.; Wetzel, R. Polyglutamine aggregation behavior in vitro supports a recruitment mechanism of cytotoxicity. *J. Mol. Biol.* **2001**, *311*, 173−182.
(40) Thakur, A.; Wetzel, R. Mutational analysis of the structural organization of polyglutamine aggregates. *Proc. Natl. Acad. Sci. U.S.A.* **2002**, *99*, 17014−17019.

AR050069H